Jui-Tang Tseng
Graduate Student

Chung-Biau Tsay[1]
Professor

Department of Mechanical Engineering,
National Chiao Tung University, Hsinchu, Taiwan
30010, Republic of China

Mathematical Model and Surface Deviation of Cylindrical Gears With Curvilinear Shaped Teeth Cut by a Hob Cutter

The generating motion of a cylindrical gear with curvilinear shaped teeth cut by a CNC hobbing machine is proposed. On the basis of the cutting mechanism and the gear theory, the surface equation of this type of gear is developed as a function of hob cutter design parameters. Computer graphs of the curvilinear-tooth gear are presented based on the developed gear's mathematical model, and the tooth surface deviations due to machine-tool settings with nominal radius of circular tooth traces are also investigated. [DOI: 10.1115/1.1876437]

1 Introduction

Helical gears are widely used as parallel-axis power transmission devices, however they transmit power with axial thrust forces. The cylindrical gear with curvilinear shaped teeth transmits power without inducing axial thrust forces, therefore, this kind of gear can be considered to substitute the helical gear. Liu [1] proposed the manufacture of the cylindrical gear with curvilinear shaped teeth by a face mill-cutter with a special machine, and stated that the merits of curvilinear-tooth gears included higher bending strength, lower noise, better lubrication effect, and no axial thrust force. Dai et al. [2] proposed the manufacture of a cylindrical gear with curved teeth by a CNC hobbing machine with an attachment for the hob head, male and female flying cutters. Tseng and Tsay [3] considered an imaginary rack cutter with a curved-tooth to develop the mathematical model of cylindrical gears with curvilinear shaped teeth, and investigated the tooth undercutting of curvilinear-tooth gears. Andrei et al. [4] developed a special cutting tool to generate the curved face width gears for nonmetallic materials.

Owing to easy tool settings, high efficiency and reliable quality, hob cutters have been widely used for manufacturing a variety of gears such as spur, helical, and worm gears. A hob cutting mechanism is a mechanism with multiple degrees of freedom in the process of gear generation. Chang et al. [5] proposed a general gear mathematical model simulating the generation process of a 6-axis CNC hobbing machine when the hob's swivel axis is fixed. Litvin and Seol [6] investigated the necessary and sufficient conditions of the envelope for a two-parameter family of surfaces.

It is not easy to manufacture curvilinear-tooth gears by using an ordinary hobbing machine. When the curvilinear-tooth gear is generated by a hob cutter, the hob rotates with an angular velocity ω about the hob's swivel axis, and the revolution center of the hob's swivel translates with a velocity υ along the worktable axis. However, the linear velocity υ correlates with angular velocity ω.

In this study, the authors first set up the cutting mechanism of a CNC hobbing machine and develop the mathematical model of a hob cutter. According to the cutting mechanism, the kinematic relationship between the hob cutter and work piece can be obtained. The mathematical model of the curvilinear-tooth gear hobbing simulation for a 6-axis CNC hobbing machine can be developed based on the proposed cutting mechanism, generation concept with multiple degrees of freedom, and theory of mechanisms. Using computer graphics, a three-dimensional tooth surface of curvilinear-tooth gears can be plotted. In addition to developing a mathematical model for cylindrical gears with curvilinear shaped teeth cut by a hob cutter, this study investigates the relationship between tooth surface deviations and machine-tool settings. The proposed mathematical model, which is capable of simulating the gear cutting process for the CNC hobbing with a hob cutter, can facilitate gear manufacturers to design and manufacture curvilinear-tooth gears.

2 Generation Method of Curvilinear-Tooth Gear

Figure 1 depicts a schematic drawing of a 6-axis CNC hobbing machine, where axes X, Z, and Y represent the functions of the radial feed, axial feed and hob shift of the hob cutter, respectively; Axes A, B, and C are the hob's swivel axis, hob's spindle axis and worktable axis, respectively. Some axes of the CNC hobbing machine are fixed while some axes rotate with a specific relationship during the manufacturing process. For example, in the manufacturing of helical and spur gears, axes X and A are fixed and in the manufacturing of worm gears, axes A, X, and Z are fixed.

Figure 2 illustrates the generating method of a curvilinear-tooth gear cut by hob cutters. Axes Z_h and Z_f are the rotation axis of hob cutter and work piece, respectively. Point O_f is located on the middle section of a work piece width. O_h denotes the rotational center of the hob's swivel. Circular-arc $\widehat{MN}$ stands for the tooth traces of the curvilinear-tooth gear, O_e indicates the center of circular arc $\widehat{MN}$, and R represents the nominal radius of circular tooth trace.

In addition to a rotation motion about axis Z_h for the hob's spindle, the rotation center of the hob's swivel O_h translates along axis Z_f and the swivel axis rotates about point O_h. The rotational angle of the hob's swivel and the axial feed displacement motion are designated with ϕ_A and l_z. They are related with the equation:

$$l_z = |\overline{QO_h}| = R \sin \phi_e = R \sin(\phi_A + \beta), \tag{1}$$

where β is the lead angle of the hob cutter. Differentiating Eq. (1) with respect to time, the relationship between the linear velocity of axial feed motion $\mathbf{V}_z$ and the angular velocity of hob's swivel ω_A can be expressed as follows:

$$\mathbf{V}_z = -\frac{dl_z}{dt}\mathbf{k}_f = -\omega_A R \cos(\phi_A + \beta)\mathbf{k}_f. \tag{2}$$

[1]Author to whom correspondence should be addressed.

Contributed by the Power Transmission and Gearing Committee for publication in the JOURNAL OF MECHANICAL DESIGN. Manuscript receieved June 7, 2004; revised October 7, 2004. Associate Editor: D. Dooner.

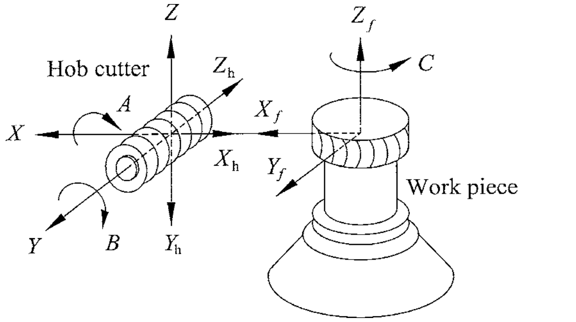

Fig. 1 A schematic drawing of a 6-axis CNC hobbing machine

The hob and work piece perform related rotation with respect to their own axes. The relationship of rotational angles between the work piece and hob can be represented as follows:

$$\phi_2 = \frac{T_1}{T_2}\phi_B + \Delta\phi_2. \tag{3}$$

where ϕ_2 and ϕ_B denote rotational angles of the work piece and the spindle of hob cutter. T_1 and T_2 are the number of threads of the hob cutter and the number of teeth of the generated gear, respectively. $\Delta\phi_2$ represents an additional angle of work piece rotation due to feed motion of the hob. According to Fig. 2, the additional angle for cutting curvilinear-tooth gears can be represented by:

$$\Delta\phi_2 = \frac{R(1-\cos(\phi_A+\beta))}{r_2}, \tag{4}$$

where r_2 indicates the radius of operating pitch cylinder of the work piece. Differentiating Eq. (3) with respect to time, then the relationship of angular velocity among ω_A, ω_B and ω_2 can be obtained as follows:

$$\omega_2 = \frac{T_1}{T_2}\omega_B + \frac{R\sin(\phi_A+\beta)}{r_2}\omega_A. \tag{5}$$

Equation (5) represents the work piece rotation ω_2 in terms of two independent variables ω_A and ω_B. To generate the curvilinear-tooth gears by a hob cutter, axes A, B, C, and Z of a hobbing machine must be controllable in the process of gear generation.

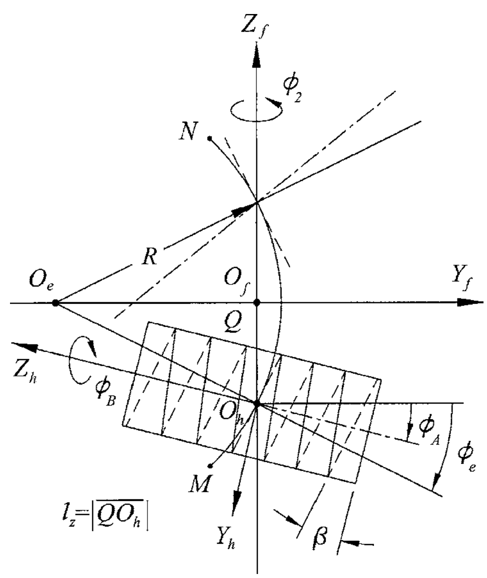

Fig. 2 Generating method of a curvilinear-tooth gear cut by hob cutters

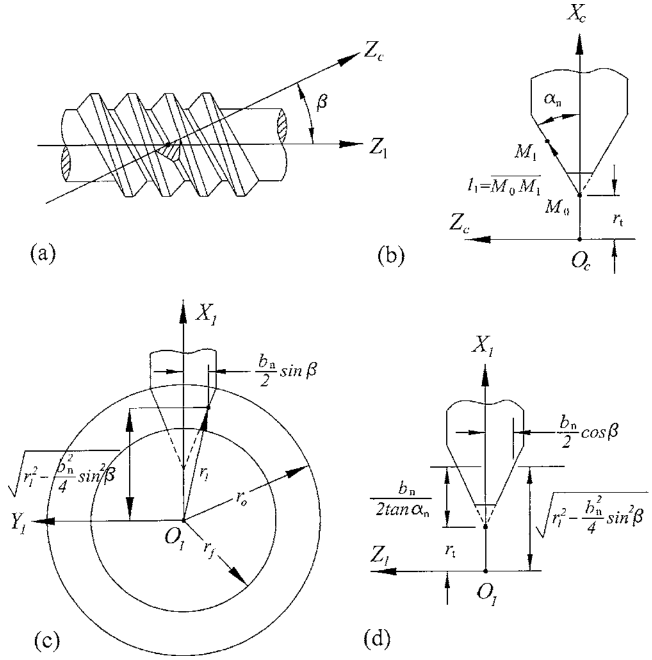

Fig. 3 Geometry of the straight-edged cutting blade and worm-type hob cutter

3 Equation of the Hob Cutter

The tooth profile of the gears is generated as an involute curve by using a ZI worm-type hob cutter, but the axial and normal profiles of the ZI worm-type hob are curvilinear shapes. It is more difficult to manufacture and measure the profiles of the ZI worm-type hob than those of other types of hobs. The axial profile of the ZA worm-type hob and the normal profile of the ZN worm-type hob are straight-lined shapes. These types of hobs are easier to manufacture the profiles at axial or normal section with straight-lined shapes. Therefore, the ZA worm-type or ZN worm-type hobs are chosen instead of the ZI worm-type hob for generation of involute gears.

The ZN worm-type hob cutter is widely used in the gear manufacturing. A right-hand ZN worm-type hob cutter is used to simulate the manufacture of curvilinear-tooth gears in this study. The surfaces of the hob cutter can be generated by a blade with the straight lined shape, performing a screw motion with respect to the hob cutter's axis. The cutting blade is installed on the groove normal section of the ZN-type worm, as shown in Fig. 3(a). Parameter β designates the lead angle of the worm. The generating lines can be represented by a coordinate system $S_c(X_c, Y_c, Z_c)$ that is rigidly connected to the blade, as shown in Fig. 3(b), expressed by:

$$\mathbf{R}_c^{(B)} = \begin{bmatrix} r_t + l_1\cos\alpha_n \\ 0 \\ \pm l_1\sin\alpha_n \\ 1 \end{bmatrix}, \tag{6}$$

where symbol l_1 is one of the design parameters of the straight-lined cutting blade surface which represents the distance measured from the initial point M_o, moving along the straight line $\overline{M_oM_1}$, to any point M_1 on X_c–Z_c section of the cutting blade surface. Design parameter α_n symbolizes the half-apex blade angle formed by the straight-lined blade and X_c-axis, as illustrated in Fig. 3(b). In Eq. (6), the upper sign represents the left-side cutting blade while the lower sign indicates the right-side cutting blade. In Fig. 3(c), the symbols r_o, r_1, and r_f represent the outside radius, pitch radius, and root radius of the ZN type-worm hob cutter, respec-

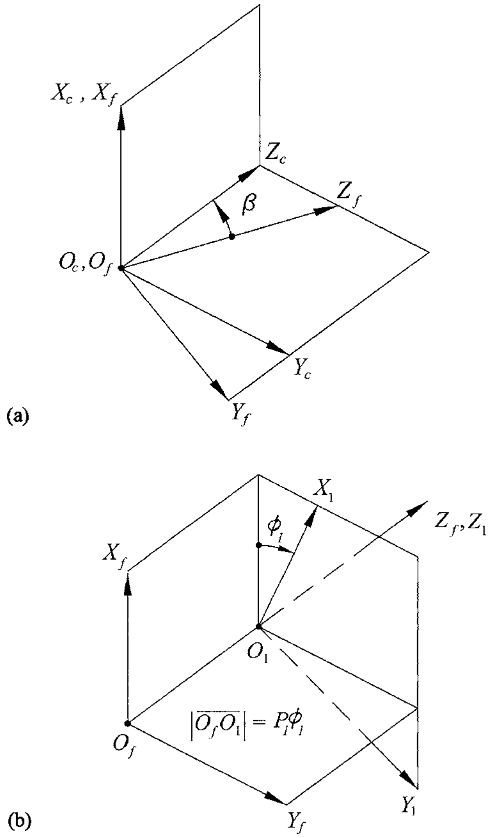

Fig. 4 Relations between the hob cutter and cutting blade coordinate systems. (*a*) Relationship between coordinate systems S_c and S_f. (*b*) Relationship between coordinate systems S_1 and S_f.

tively. The cutting blade width b_n equals the normal groove width of the hob cutter. Then, the design parameter r_t can be obtained from Figs. 3(*c*) and 3(*d*) as follows:

$$r_t = \sqrt{r_1^2 - \frac{b_n^2}{4}\sin^2\beta} - \frac{b_n}{2\tan\alpha_n}. \tag{7}$$

Figure 4 shows the relations among coordinate systems $S_c(X_c, Y_c, Z_c)$, $S_1(X_1, Y_1, Z_1)$, and $S_f(X_f, Y_f, Z_f)$, where coordinate system S_c is the blade coordinate system, coordinate system S_1 is rigidly connected to the hob cutter's surface, and coordinate system S_f is the reference coordinate system. Axes Z_c and Z_f form an angle β that is equal to the lead angle on the worm pitch cylinder as shown in Fig. 4(*a*). Figure 4(*b*) shows that the movable coordinate system S_1 performs a screw motion with respect to the fixed coordinate system S_f. Z_1-axis is the rotation axis of the hob cutter. The locus of the cutting blade can be represented in coordinate system S_1 by applying the following homogeneous coordinate transformation matrix equation:

$$\mathbf{R}_1^{(1)} = \mathbf{M}_{1f}\mathbf{M}_{fc}\mathbf{R}_c^{(B)}, \tag{8}$$

where

$$\mathbf{M}_{fc} = \begin{bmatrix} 1 & 0 & 0 & 0 \\ 0 & \cos\beta & -\sin\beta & 0 \\ 0 & \sin\beta & \cos\beta & 0 \\ 0 & 0 & 0 & 1 \end{bmatrix},$$

and

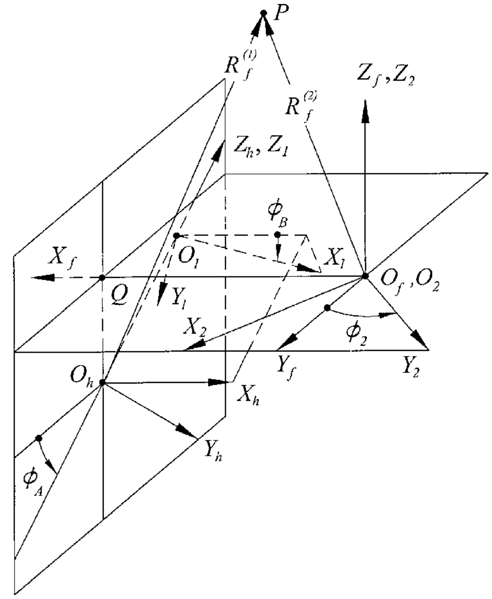

Fig. 5 Coordinate systems of the hob cutter and CNC hobbing machine

$$\mathbf{M}_{1f} = \begin{bmatrix} \cos\phi_1 & \sin\phi_1 & 0 & 0 \\ -\sin\phi_1 & \cos\phi_1 & 0 & 0 \\ 0 & 0 & 1 & -P_1\phi_1 \\ 0 & 0 & 0 & 1 \end{bmatrix},$$

where P_1 denotes the lead-per-radian revolution of the hob cutter's surface, and ϕ_1 indicates the rotational angle of the hob cutter in relevant screw motion. Substituting Eq. (6) into Eq. (8), the surface equation of the ZN worm-type hob cutter $\mathbf{R}_1^{(1)}$, represented in coordinate system S_1, can be obtained:

$$\mathbf{R}_1^{(1)}(l_1, \phi_1) = \begin{bmatrix} (r_t + l_1\cos\alpha_n)\cos\phi_1 \mp l_1\sin\alpha_n\sin\phi_1\sin\beta \\ -(r_t + l_1\cos\alpha_n)\sin\phi_1 \mp l_1\sin\alpha_n\cos\phi_1\sin\beta \\ \pm l_1\sin\alpha_n\cos\beta - P_1\phi_1 \\ 1 \end{bmatrix}, \tag{9}$$

where l_1 and ϕ_1 are the surface parameters of the hob cutter. In Eq. (9), the upper sign represents the right-side hob cutter surface while the lower sign indicates the left-side hob cutter surface.

The surface normal vector $\mathbf{N}_1^{(1)}$ of the hob cutter can be obtained and represented in coordinate system S_1 as follows:

$$\mathbf{N}_1^{(1)} = \frac{\partial\mathbf{R}_1^{(1)}}{\partial l_1} \times \frac{\partial\mathbf{R}_1^{(1)}}{\partial\phi_1}, \tag{10}$$

where

$$\frac{\partial\mathbf{R}_1^{(1)}}{\partial l_1} = \begin{bmatrix} \cos\alpha_n\cos\phi_1 \mp \sin\alpha_n\sin\phi_1\sin\beta \\ -\cos\alpha_n\sin\phi_1 \mp \sin\alpha_n\cos\phi_1\sin\beta \\ \pm\sin\alpha_n\cos\beta \end{bmatrix},$$

and

$$\frac{\partial\mathbf{R}_1^{(1)}}{\partial\phi_1} = \begin{bmatrix} -(r_t + l_1\cos\alpha_n)\sin\phi_1 \mp l_1\sin\alpha_n\cos\phi_1\sin\beta \\ -(r_t + l_1\cos\alpha_n)\cos\phi_1 \pm l_1\sin\alpha_n\sin\phi_1\sin\beta \\ -P_1 \end{bmatrix}.$$

4 Relative Velocity and Equation of Meshing Between Hob Cutter and Work Piece

Figure 5 reveals the schematic relationship among coordinate systems S_1, S_h, S_2, and S_f for the gear generation mechanism. Coordinate system S_1 is attached to the hob cutter while coordinate system S_2 is attached to the gear blank. Coordinate system S_h is the reference coordinate system and coordinate system S_f is the fixed coordinate system attached to the machine housing. Symbols ϕ_B and ϕ_2 are rotational angles of the hob cutter and gear blank, respectively. ϕ_A depicts the rotational angle of hob's swivel axis.

The homogeneous coordinate transformation matrix $\mathbf{M}_{ij}$ transforms the coordinates from coordinate system S_j to S_i. According to the relations as illustrated in Fig. 5, matrices $\mathbf{M}_{h1}$, $\mathbf{M}_{fh}$, and $\mathbf{M}_{2f}$ can be obtained as follows:

$$\mathbf{M}_{h1} = \begin{bmatrix} \cos\phi_B & -\sin\phi_B & 0 & 0 \\ \sin\phi_B & \cos\phi_B & 0 & 0 \\ 0 & 0 & 1 & l_h \\ 0 & 0 & 0 & 1 \end{bmatrix}, \quad (11)$$

$$\mathbf{M}_{fh} = \begin{bmatrix} -1 & 0 & 0 & l_x \\ 0 & -\sin\phi_A & -\cos\phi_A & 0 \\ 0 & -\cos\phi_A & \sin\phi_A & -l_z \\ 0 & 0 & 0 & 1 \end{bmatrix}, \quad (12)$$

and

$$\mathbf{M}_{2f} = \begin{bmatrix} \cos\phi_2 & \sin\phi_2 & 0 & 0 \\ -\sin\phi_2 & \cos\phi_2 & 0 & 0 \\ 0 & 0 & 1 & 0 \\ 0 & 0 & 0 & 1 \end{bmatrix}, \quad (13)$$

where

$$l_h = |\overline{O_1O_h}|, \; l_x = |\overline{O_fQ}|, \quad \text{and } l_z = |\overline{QO_h}|.$$

In Fig. 5, point P is a common point to both hob cutter and work piece. The surface coordinates of the hob cutter can be transformed to the fixed coordinate system S_f as follows:

$$\mathbf{R}_f^{(2)} = \overline{O_fP} = \mathbf{M}_{fh}\mathbf{M}_{h1}\mathbf{R}_1^{(1)} = x_f\mathbf{i}_f + y_f\mathbf{j}_f + z_f\mathbf{k}_f. \quad (14)$$

The velocity of point P attached to the work piece can be obtained by:

$$\mathbf{V}_f^{(2)} = \boldsymbol{\omega}_2 \times \mathbf{R}_f^{(2)} = -y_f\omega_2\mathbf{i}_f + x_f\omega_2\mathbf{j}_f, \quad (15)$$

where $\boldsymbol{\omega}_2 = \omega_2\mathbf{k}_f$ indicates the angular velocity of the work piece. The velocity of point P attached to the hob cutter can be represented as follows:

$$\mathbf{V}_f^{(1)} = (\boldsymbol{\omega}_A + \boldsymbol{\omega}_B) \times \mathbf{R}_f^{(1)} + \mathbf{V}_z, \quad (16)$$

where

$$\boldsymbol{\omega}_A = -\omega_A\mathbf{i}_f,$$

$$\boldsymbol{\omega}_B = -\omega_B\cos\phi_A\mathbf{j}_f + \omega_B\sin\phi_A\mathbf{k}_f,$$

and

$$\mathbf{R}_f^{(1)} = \mathbf{R}_f^{(2)} - (l_x\mathbf{i}_f - l_z\mathbf{k}_f) = (x_f - l_x)\mathbf{i}_f + y_f\mathbf{j}_f + (z_f + l_z)\mathbf{k}_f.$$

After some mathematical operations, Eq. (16) can be simplified as follows:

$$\mathbf{V}_f^{(1)} = \begin{bmatrix} -(z_f + l_z)\omega_B\cos\phi_A - y_f\omega_B\sin\phi_A \\ (x_f - l_x)\omega_B\sin\phi_A + (z_f + l_z)\omega_A \\ -y_f\omega_A + (x_f - l_x)\omega_B\cos\phi_A - R\omega_A\cos(\phi_A + \beta) \end{bmatrix}. \quad (17)$$

Based on Eqs. (15) and (17), the relative velocity $\mathbf{V}_f^{(12)}$ represented in the coordinate system S_f can be expressed by:

$$\mathbf{V}_f^{(12)} = \mathbf{V}_f^{(1)} - \mathbf{V}_f^{(2)} = \begin{bmatrix} -(z_f + l_z)\omega_B\cos\phi_A - y_f\omega_B\sin\phi_A + y_f\omega_2 \\ (x_f - l_x)\omega_B\sin\phi_A + (z_f + l_z)\omega_A - x_f\omega_2 \\ -y_f\omega_A + (x_f - l_x)\omega_B\cos\phi_A - R\omega_A\cos(\phi_A + \beta) \end{bmatrix}. \quad (18)$$

Equation (18) shows the relative velocity of the hob cutter and the work piece at their common point P. The common surface normal $\mathbf{N}_f^{(1)}$ is perpendicular to the relative velocity $\mathbf{V}_f^{(12)}$. Therefore, the following equation must be observed [7]:

$$\mathbf{N}_f^{(1)} \cdot \mathbf{V}_f^{(12)} = f(l_1, \phi_1, \phi_A, \phi_B, \phi_2(\phi_A, \phi_B)) = 0. \quad (19)$$

Equation (19) is the equation of meshing of the gear and hob cutter. This equation guarantees the tangency of the hob and the gear at any instant during the gear generating process. Substituting Eqs. (10) and (18) into Eq. (19) yields:

$$\begin{aligned}(-(z_f + l_z)\omega_B\cos\phi_A - y_f\omega_B\sin\phi_A + y_f\omega_2)n_{xf} + ((x_f - l_x)\omega_B\sin\phi_A \\ + (z_f + l_z)\omega_A - x_f\omega_2)n_{yf} + (-y_f\omega_A + (x_f - l_x)\omega_B\cos\phi_A \\ - R\omega_A\cos(\phi_A + \beta))n_{zf} = 0,\end{aligned} \quad (20)$$

where n_{xf}, n_{yf}, and n_{zf} symbolize the components of the unit normal vector. Substituting Eq. (5) into Eq. (20) and rearranging in terms of two independent variables, ω_A and ω_B, yields the following equation:

$$\begin{aligned}&\omega_B\left[\left(-(z_f + l_z)\cos\phi_A - y_f\sin\phi_A + y_f\frac{T_1}{T_2}\right)n_{xf} + \left((x_f - l_x)\sin\phi_A \right.\right. \\ &\left.\left. - x_f\frac{T_1}{T_2}\right)n_{yf} + (x_f - l_x)\cos\phi_A n_{zf}\right] + \omega_A\left[y_f\frac{R\sin(\phi_A + \beta)}{r_2}n_{xf} \right. \\ &\left. + \left(z_f + l_z - x_f\frac{R\sin(\phi_A + \beta)}{r_2}\right)n_{yf} + (-y_f - R\cos(\phi_A + \beta))n_{zf}\right] \\ &= 0.\end{aligned} \quad (21)$$

Since ω_A and ω_B are independent variables, two equations of meshing are obtained and can be represented in coordinate system S_f as follows:

$$\begin{aligned}f_A(l_1, \phi_1, \phi_A, \phi_B, \phi_2(\phi_A, \phi_B)) &= y_f\frac{R\sin(\phi_A + \beta)}{r_2}n_{xf} + \left(z_f + l_z \right. \\ &\left. - x_f\frac{R\sin(\phi_A + \beta)}{r_2}\right)n_{yf} + (-y_f \\ &- R\cos(\phi_A + \beta))n_{zf} \\ &= 0,\end{aligned} \quad (22)$$

$$\begin{aligned}f_B(l_1, \phi_1, \phi_A, \phi_B, \phi_2(\phi_A, \phi_B)) &= \left(-(z_f + l_z)\cos\phi_A - y_f\sin\phi_A \right. \\ &\left. + y_f\frac{T_1}{T_2}\right)n_{xf} + \left((x_f - l_x)\sin\phi_A \right. \\ &\left. - x_f\frac{T_1}{T_2}\right)n_{yf} + (x_f - l_x)\cos\phi_A n_{zf} \\ &= 0.\end{aligned} \quad (23)$$

Equations (22) and (23) are the equations of meshing that relate the surface parameters to the cutting motion parameters.

5 Mathematical Model of the Curvilinear-Tooth Gear

The surface equation of the curvilinear-tooth gear is derived as the envelope to the two-parameter family of hob thread surfaces. The locus of hob cutter surface, expressed in coordinate system S_2, can be obtained by applying the following homogeneous coordinate transformation matrix equation:

Table 1 Some major design parameters for cylindrical gears with curvilinear shaped teeth

	Hob cutter	Curvilinear-tooth gear
Number of teeth	1	25
Normal module	3	3
Normal pressure angle	25 deg	25 deg
Lead angle	2.866 deg	⋯
Face width	⋯	60 mm
Nominal radius of circular tooth trace	⋯	100 mm
Radius of pitch	30 mm	37.5 mm
Outside radius	33.75 mm	40.5 mm

$$\mathbf{R}_2^{(1)} = \mathbf{M}_{2f}\mathbf{M}_{fh}\mathbf{M}_{h1}\mathbf{R}_1^{(1)}. \quad (24)$$

According to the gear theory [7], the mathematical model of the generated gear tooth surfaces is the combination of the equation of meshing and the locus of hob cutter surfaces. Hence, the mathematical model of the gear tooth surfaces can be obtained by considering Eqs. (22)–(24), simultaneously.

6 Computer Graphs of the Curvilinear-Tooth Gear

The tooth surface equation proposed herein for curvilinear-tooth gears can be verified by plotting the gear profile. The coordinates of the curvilinear-tooth gear surface points can be calculated by solving the developed gear mathematical model using numerical methods.

Table 1 lists some major design parameters of a curvilinear-tooth gear. Based on the developed gear mathematical model, a three-dimensional tooth profile of the curvilinear-tooth gear is plotted as displayed in Fig. 6. The figure shows that the right- and left-side tooth surfaces of a curvilinear-tooth gear are convex and concave teeth, respectively.

7 Surface Deviations of Curvilinear-Tooth Gear

The gear design parameters are chosen the same as those listed in Table 1. Figure 7 shows the tooth profile of the curvilinear-tooth gear generated by nominal radii of circular tooth trace $R = 100$ mm, 120 mm, and 200 mm at cross section $Z_2=0$ mm and $Z_2=30$ mm, respectively. The tooth profiles generated by a hob cutter with different nominal radius of circular tooth trace are the same at the cross section $Z_2=0$ mm as illustrated in Fig. 7(*a*). The proposed curvilinear-tooth gear can be viewed as the gear with varying helical angle across the whole face width, and helical angle at the cross section $Z_2=0$ mm is zero. Therefore, the tooth profiles of the curvilinear-tooth gear generated by different R at cross section $Z_2=0$ mm is the same as that of spur gears. The results illustrated in Fig. 7(*a*) verify that the mathematical models proposed herein are correct. Figure 7(*b*) shows the tooth profiles generated by a hob cutter with different R are not the same at the cross section $Z_2=30$ mm.

Figure 8 reveals the transverse chordal thickness deviations of the curvilinear-tooth gear generated by nominal radii of circular tooth trace $R=100$ mm, 120 mm, and 200 mm, respectively. It is

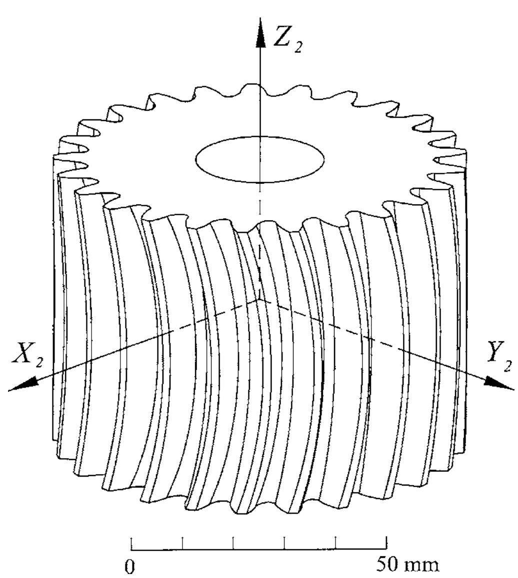

Fig. 6 Computer graph of the curvilinear-tooth gear

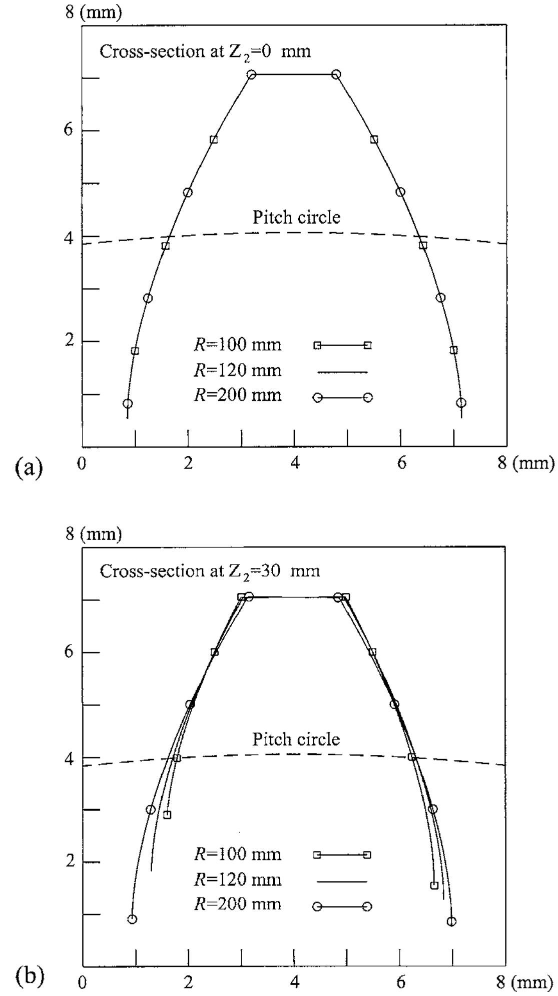

Fig. 7 Different tooth profiles of the curvilinear-tooth gear generated by R=100 mm, 120 mm, and 200 mm

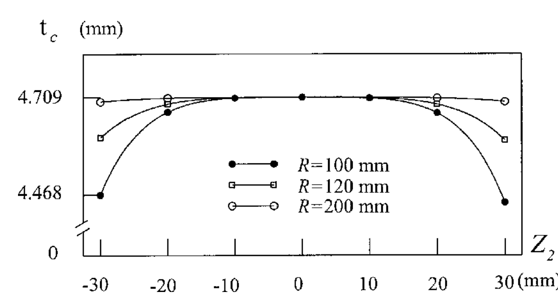

Fig. 8 Transverse chordal thickness on a different cross section

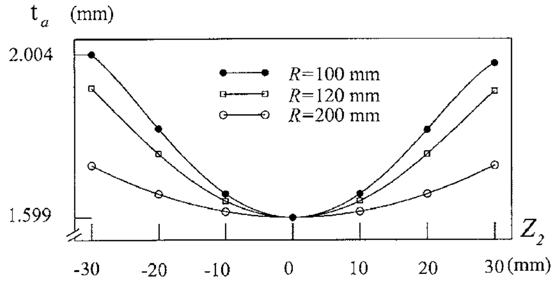

Fig. 9 Thickness of tooth at addendum circle on a different cross section

found that the transverse chordal thickness at the middle section of face width, i.e., t_c=4.709 mm, is larger than those at other sections. A smaller R results in a smaller transverse chodal thickness at the ends of face width as shown in Fig. 8. Figure 9 illustrates the relationship between the Z_2 component of the tooth cross-section and the thickness of tooth at the addendum circle. It reveals that the tooth thickness at the middle section of face width, i.e., t_a=1.599 mm, is smaller than those at other sections, and a smaller R induces a larger tooth thickness t_a at the ends of face width.

The tooth thickness of the curvilinear-tooth gear generated by hob cutters with different nominal radii of circular tooth trace are the same at the middle section of the tooth flank, i.e., Z_2=0 mm. The analysis results shown in Figs. 8 and 9 indicated that the tooth thicknesses, t_c and t_a, at the extreme ends of the face width approach that at the middle section of the face width when the nominal radius of circular tooth trace R is increased.

It is noted that the herringbone gears are in line contact, however, the curvilinear-tooth gear pair proposed herein is in point contact. Therefore, the advantage of the proposed gear pair is not sensitive to the axial misalignments. According to the analysis result shown in Fig. 8, the curvilinear shapes of the teeth are similar to those of crowned tooth surfaces. Thus, the edge contact of the curvilinear-tooth gears can be avoided.

8 Conclusion

The mathematical model of curvilinear-tooth gears has been developed on the basis of the CNC hobbing machine cutting mechanism. The model is represented as a function of hob design parameters and generating motion parameters. The developed mathematical model provides the industry with an efficient method to design and manufacture curvilinear-tooth gears. The illustrated approach can be further extended to derive the mathematical model of noncircular face width gears, for example, parabolic or elliptical curved tooth traces.

The tooth surface deviations induced by different nominal radii of circular tooth traces are also investigated. The transverse gear chordal thickness measured at the middle section is larger than those of other sections, but the tooth thickness at the addendum circle in the middle section of the face width is smaller than those of other sections. The developed tooth mathematical model helps to explore the possibility for further investigations, such as sensitivity, kinematic errors and contact stress analyses.

Acknowledgments

The authors are grateful to the National Science Council of the R.O.C. for the grant. Part of this work was performed under Contract No. NSC 92-2212-E-009-032. The authors would also like to express their sincere thanks to Professor Y. Ariga and Emeritus Professor S. Nagata of Nippon Institute of Technology for their valuable suggestions.

References

[1] Liu, S. T., 1988, "Curvilinear Cylindrical Gears," Gear Technol., **5**(3), pp. 8–12.
[2] Dai, Y., Ariga, Y., and Nagata, S., 1999, "Study on A Cylindrical Gear with Curved Tooth Traces," Tenth World Congress on The Theory of Machine and Mechanisms, Vol. 6, pp. 2337–2342.
[3] Tseng, R. T., and Tsay, C. B., 2001, "Mathematical Model and Undercutting of Cylindrical Gears with Curvilinear Shaped Teeth," Mech. Mach. Theory, **36**, pp. 1189–1202.
[4] Andrei, L., Andrei, G, Epureanu, A., Oancea, N., and Walton, D., 2002, "Numerical Simulation and Generation of Curved Face Width Gears," Int. J. Mach. Tools Manuf., **42**, pp. 1–6.
[5] Chang, S. L., Tsay, C. B., and Nagata, S., 1997, "A General Mathematical Model of Gears Cut by CNC Hobbing Machines," ASME J. Mech. Des., **119**, pp. 180–113.
[6] Litvin, F. L., and Seol, I. H., 1996, "Computerized Determination of Gear Tooth Surface as Envelope to Two Parameter Family of Surfaces," Comput. Methods Appl. Mech. Eng., **138**, pp. 213–225.
[7] Litvin, F. L., 1994, *Gear Geometry and Applied Theory*, PTR Prentice–Hall, New Jersey.